FATIGUE AND HYSTERESIS EFFECTS IN WOOD-BASED PANELS UNDER CYCLIC SHEAR LOAD THROUGH THICKNESS

Takanori Sugimoto

Graduate Student
Graduate School of Bioagricultural Sciences
Nagoya University
Chikusa, 464-8601 Nagoya, Japan

Mariko Yamasaki

Graduate Student
Graduate School of Engineering
Nagoya Institute of Technology
Showa, 466-8555 Nagoya, Japan

and

Yasutoshi Sasaki

Associate Professor
Graduate School of Bioagricultural Sciences
Nagoya University
Chikusa, 464-8601 Nagoya, Japan

(Received March 2005)

ABSTRACT

The fatigue behavior of wood-based panels (plywood: PW, and oriented strandboard: OSB) under cyclic shear load through the thickness was experimentally investigated. Test specimens were cut into sections of 350-mm length and 240-mm width. Pulsating shear load through the thickness was applied along the length of specimens at stress levels corresponding to 60%~100% of static strength. The hysteresis loops of stress-strain curves were determined by measuring the shear load and the shear strain at the center of the specimen surface throughout the fatigue tests. The area enclosed by a hysteresis loop was defined as the energy loss per cycle, and was obtained for each loading cycle. To discuss the fatigue properties of wood-based panels under shear load through the thickness, the energy loss per cycle was examined in relation to the number of loading cycles. The energy loss per cycle at each stress level showed an almost constant value throughout most of the fatigue life, that is, from 5~10 loading cycles to just before fatigue failure. A significant correlation between energy loss during 5~10 loading cycles and fatigue life was obtained. Therefore, fatigue life could be predicted by monitoring energy loss in the cyclic shear-through-thickness test with approximately 10 loading cycles. As fatigue life lengthened, mean energy loss per cycle was found to decrease and seemed to gradually approach a threshold value. The stress level at which mean energy loss per cycle is equal to the threshold value can be regarded as the fatigue limit. A model equation for the relationship between mean energy loss per cycle and fatigue life was proposed and fitted to the data obtained. The threshold values of mean energy loss per cycle for PW and OSB were found to be 0.446 and 0.350 [kJ/m^3/cycle], respectively. The fatigue limit was estimated to be approximately 40% of the static strength for PW and OSB, respectively, on the basis of the nonlinear relationship between mean energy loss per cycle and stress level.

Keywords: Energy loss, fatigue life, fatigue limit, shear through thickness, wood-based panel.

INTRODUCTION

Wood-based panels are widely used for various applications such as flooring, bearing walls, and complex beams of residential buildings. These panels are used as the sheathing of timber framing in bearing walls, and as the web in complex beams. In these cases, wood-based panels are frequently subjected to shear load along their edges, due to wind and seismic forces during

service. Frequent shear load may deteriorate the mechanical properties of wood-based panels such as shear strength and shear rigidity, and hence affect the performance of the structures. Consequently, it is important to demonstrate the fatigue behavior of these panels under shear load along their edge.

The mechanical property of shear deformation of the panel due to shearing force applied along the edge of the panel is called "shear through thickness." The shear-through-thickness property of wood-based panels is mainly determined by the two-rail shear test or edgewise shear test. For example, Shrestha (1999) reported the static shear-through-thickness properties determined by the modified two-rail shear test for oriented strandboard panels. Suzuki and Miyagawa (2003) compared the static shear-through-thickness properties of oriented strandboard (OSB), particleboard (PB), medium-density fiberboard (MDF), and plywood (PW) by the edgewise shear test, and showed that OSB has the highest shear modulus and MDF has the highest shear strength. Similar studies were also conducted using the 4 types of panels mentioned above, waferboard, and hardboard (Lee and Stephens 1988; Falk et al. 1999). It was found, from those studies, that hardboard shows superior static strength in the edgewise shear test among these 6 types of panels. Thus, there have been several studies on the static properties of wood-based panels under shear load through the thickness. On the other hand, the fatigue behaviors of these panels in shear through thickness have rarely been examined, whereas those in bending have been widely studied and many valuable results have already been reported (Bonfield et al. 1994; Bao and Eckelman 1995; Bao et al. 1996; Pritchard et al. 2001a, 2001b; Thompson et al. 2002). It is, therefore, essential to clarify the fatigue behavior of wood-based panels under shear load through the thickness. Information on the fatigue properties of these panels could be useful for the structural design of timber construction and the development of new wood composite materials.

In the fatigue test for wood and wood composites, a hysteresis loop is generally obtained for each cycle of repeated loading. The area enclosed by the hysteresis loop corresponds to the dissipated strain energy. Okuyama et al. (1984) studied the tensile and compressive fatigue of solid wood and reported that the average energy loss per cycle consists of two parts, that is, the energy loss not concerned with fractures and that concerned with fractures. Then, Kohara and Okuyama (1993) showed in the study on tensile fatigue of solid wood that the former is related to linear viscoelasticity and independent of the number of loading cycles, and that the latter is related to minute damages and varies with repeated loadings. Energy loss is considered to reflect the fatigue damage and is analyzed in other studies (Hacker and Ansell 2001; Pritchard et al. 2001b; Sasaki et al. 2005). Therefore, characteristic analysis based on energy loss will provide important knowledge about the damage development and fatigue mechanism in cyclic shear through thickness of wood-based panels.

The purpose of this study is to demonstrate the fatigue behavior of wood-based panels under shear load through the thickness. Two types of panels were subjected to repeated shear load through the thickness. Hysteresis loops were measured throughout the fatigue test, and the change of energy loss with cyclic loading was analyzed. Especially, the estimation of the fatigue life and fatigue limit of these panels was discussed based on the energy loss.

MATERIALS AND METHODS

Specimen preparation

The commercially available wood-based panels used in this study are listed in Table 1. The plywood manufactured by Toyo Plywood Co., Ltd. (Nagoya, Japan) was made of Chinese larch (*Larix potaninii* Batal). Five-ply plywoods of two thicknesses were obtained: 9-mm-thick PW (PW-9) consisting of 1.5-, 2.25-, 1.5-, 2.25-, and 1.5-mm-thick veneers from the face to the back ply, and 12-mm-thick PW (PW-12) consisting of 1.75-, 3.5-, 1.5-, 3.5-, and 1.75-mm-thick veneers. The length and width of these panels were 1800 and 900 mm, respectively, and the fiber

TABLE 1. *Description of commercial panels and test specimens.*

Group	Panel type	Panel thickness [mm]	Panel grade	Density [g/cm^3]	Moisture content [%]	Number of panels	Number of specimens prepared for	
							Static test	Fatigue test
PW-9	Plywood (PW)	9	JAS structural plywood, type special, class 1, 5-ply	0.61	6.2	3	6	18
PW-12	Plywood (PW)	12	JAS structural plywood, type special, class 1, 5-ply	0.63	6.5	3	6	18
OSB-9.5	Oriented strandboard (OSB)	9.5	JAS structural panel, class 4, 4-layer	0.62	5.8	3	6	18
OSB-12	Oriented strandboard (OSB)	12	JAS structural panel, class 3, 4-layer	0.63	6.0	3	6	18

direction of face veneers was parallel to the length of panels. Alkali phenol resin glue was used as binder.

The oriented strandboard manufactured by Slocan Forest Products Ltd. (British Columbia, Canada) was made of aspen (*Populus tremuloides* Michx.). Four-layer boards of two thicknesses, 9.5-mm-thick OSB (OSB-9.5) and 12-mm-thick OSB (OSB-12), were obtained. Strands in the face layers were mainly aligned parallel to the panel length, and those in the core layers perpendicular to the panel length in both OSB-9.5 and OSB-12. The length and width of these panels were 2400 and 900 mm, respectively. Liquid phenol resin glue was used as binder in the face layers and powdered glue in the core layers.

Test specimens were prepared according to ASTM D 2719, Method C; Two Rail Shear Test (2001). Three sheets of the test panel were obtained for each group, and the peripheral edge was cut off from every side. Then, twelve 350-(length) × 240-(width) mm specimens were obtained from a panel with the shorter sides parallel to the length of the panel, as shown in Fig. 1. We designated the specimens as 1 to 6 along the panel length and L and R along the panel width in each panel. Two specimens (2R and 5L) were prepared for the static test, and six specimens (1R, 2L, 3R, 4L, 5R, and 6L) for the fatigue test. The remainder was used for the preliminary tests and as reserve. The size of the test specimens described above was smaller than the standard specimen size (610 × 406 mm) defined in ASTM D 2719 because the range of movement of the cross-yoke is under 600 mm in our test machine.

Lumber splints of African makore (*Tieghemella heckelii* A. Chev.) with the density of 0.82 g/cm^3 were bonded to the longer sides on the surface of each specimen, using resorcinol resin glue, to reinforce and hold the specimen for shear-through-thickness tests in both static and fatigue. The fiber direction of face veneers or principal orientation of the strands in face layers coincides with the shorter sides of test specimens. It is prescribed in ASTM D2719 that bolts for clamping are spaced straight on center not more than 101 mm. In the case of this study, specimen length is shorter than the standard length in ASTM D2719, as mentioned above, and a large number of loading cycles were expected in the fatigue test. Therefore, seven bolt holes were made in zigzag to fasten the splints to a pair of steel rails more firmly, as shown in Fig. 1.

Static test

In order to determine the static strength in shear through thickness of PW and OSB specimens, the static test under shear load through the thickness was first performed prior to the fatigue test. The results were used to design the fatigue test.

Six specimens were prepared for each group, as mentioned above. From these, five specimens

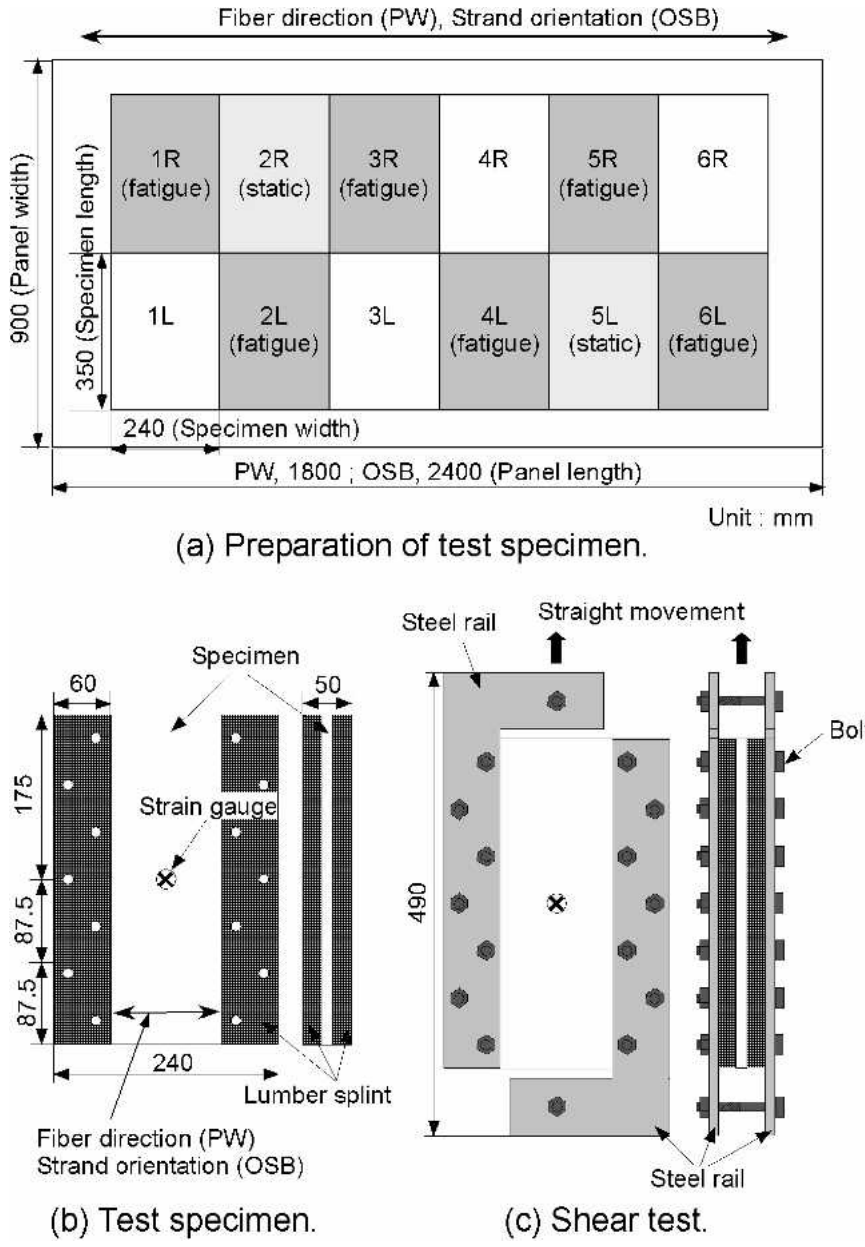

FIG. 1. Schematic illustrations of specimen preparation and shear-through-thickness test set-up.

were selected by visual inspection and used for the static test.

An electrohydraulic servo fatigue testing machine (EHF-UB5-10L, manufactured by Shimadzu Corporation, Kyoto, Japan) was used for the static test. The test was conducted according to ASTM D 2719, Method C. In this study, two pairs of L-shaped steel rails were fastened to the specimen with 14 bolts, as shown in Figs. 1(c) and 2. This fastening secured the specimen for not only the static test but also the fatigue test. As shown in Figs. 1(c) and 2, the upper rails

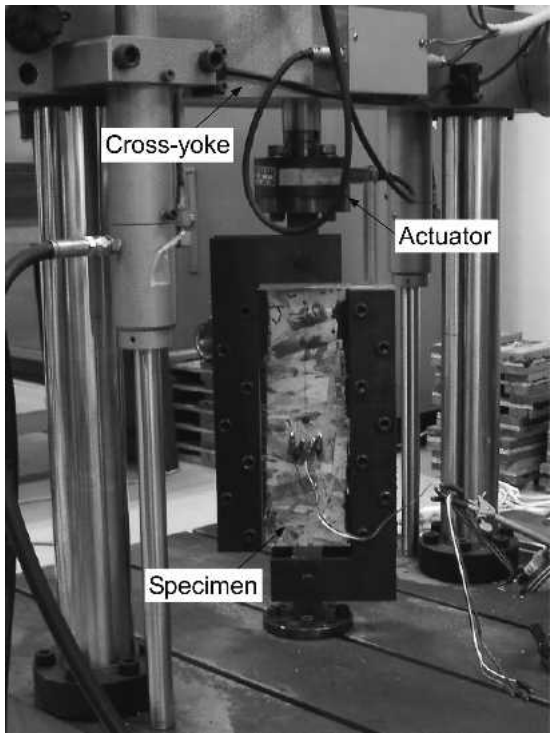

FIG. 2. Actual experimental setup for both static and fatigue shear tests.

were attached to the actuator of the test machine, and the lower rails were fixed. Shear load was applied longitudinally to the specimen.

The static test was carried out under controlled conditions at a constant displacement rate of 1.5 mm/min. Shear strain was measured at the center of the specimen surface, as shown in Figs. 1(b) and 2. The biaxial strain gauge (KFG-5-120-D16, manufactured by Kyowa Electronic Instruments Co., Ltd., Tokyo, Japan, 5-mm gauge length and 120 Ω resistance) was used. The biaxial strain gauge consisted of one axial gauge tilted +45° and another tilted −45° against the direction of load. Load and the displacement of the actuator were also measured.

The results of the static test are described below. Typical failure modes of PW and OSB are shown in Fig. 3. Both PW and OSB were observed to fail along the load line of shear force at the center region of the specimen. Almost all the specimens fractured in this manner.

The load-displacement curves and the shear

FIG. 3. Typical failure modes of PW (left) and OSB (right) specimens in static test.

stress-strain (*S-S*) curves obtained from the static shear-through-thickness tests are shown in Figs. 4 and 5. Static shear strength (τ_{max}) was evaluated for each test specimen using

$$\tau_{max} = P_{\max}/(L\,t), \tag{1}$$

where $P_{\max}$ is the maximum applied load, and L and t are the length and the thickness of each test specimen, respectively. The shear stress-strain curves were almost linear at the initial stage of loading, as shown in Fig. 5. The curve between 10% and 30% of static shear strength was regarded as the linear region in the present study, and shear rigidity (G) was evaluated using

$$G = \Delta\,\tau/2\,\Delta\,\varepsilon, \tag{2}$$

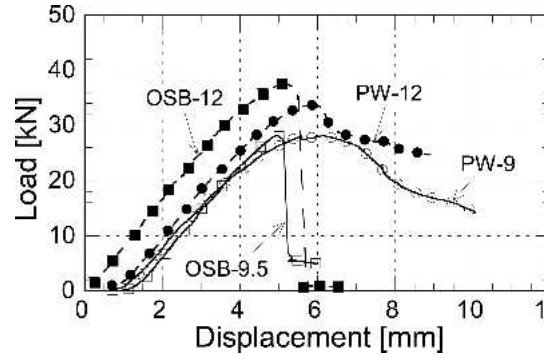

FIG. 4. Typical load-displacement relationships for each specimen obtained from static test.

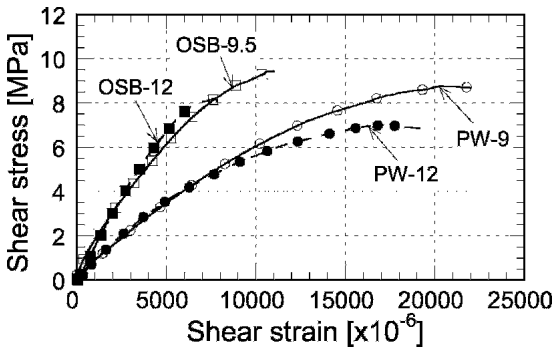

FIG. 5. Typical stress-strain relationships for each specimen obtained from static test.

where $\Delta\tau$ is the increment of shear stress between 10% and 30% of static shear strength, and $\Delta\varepsilon$ is the increment of absolute strain in the 45° direction measured with a biaxial strain gauge.

Shear strength (τ_{static}) and shear rigidity (G) obtained from the static test are listed in Table 2. The two-way repeated-measures ANOVA and post-hoc test were performed for shear strength and shear rigidity (see Table 3). ANOVA showed that there were significant differences between panel types for shear strength and shear rigidity. This result suggests that OSB specimens used in this study have higher shear performance than PW specimen used. Similar results were obtained in the edgewise shear test of wood-based panels (Lee and Stephens 1988; Suzuki and Miyagawa 2003). The mean value of static shear strength for each group was used as the reference standard of applied stress in the fatigue test.

TABLE 2. *Static strength and rigidity in shear through thickness.*

Group	n		τ_{static} [MPa]	G [GPa]
PW-9	5	Mean	9.10	0.82
		COV (%)	7.57	20.1
PW-12	5	Mean	6.82	0.90
		COV (%)	8.69	13.6
OSB-9.5	5	Mean	9.17	1.37
		COV (%)	4.45	24.5
OSB-12	5	Mean	7.98	1.14
		COV (%)	10.2	22.3

n, number of test specimens; τ_{static}, static shear strength; G, shear rigidity

TABLE 3. *Results of statistical analyses for static test.*

	p-value for τ_{static}	p-value for G
Two-way ANOVA		
Panel type	0.048*	<0.01**
Panel thickness	<0.01**	0.368
Interaction		
(Panel type − Panel thickness)	0.074	0.146
Sheffe's F test		
PW-9 vs OSB-9.5	0.998	0.012*
PW-12 vs OSB-12	0.078	0.464
PW-9 vs PW-12	<0.01*	0.968
OSB-9.5 vs OSB-12	0.069	0.428

τ_{static}, static shear strength; G, shear rigidity; *, 95% significance; **, 99% significance

Fatigue test

Fatigue testing of PW and OSB specimens under shear load through the thickness was conducted with the same experimental set-up as that for static testing.

A cyclic sinusoidal load of tension was longitudinally applied to the longer side of test specimens at the loading frequency of 0.5 Hz; this induced shear stress, as illustrated in Fig. 6. This loading frequency is in the range associated with strong wind and earthquakes (Gong and Smith 2003). Stress levels in the fatigue test were determined for each group as the ratio of applied peak stress (τ_{peak}) to static shear strength (τ_{static}) using the values shown in Table 2. Five stages equivalent to stress levels of 0.6, 0.7, 0.8, 0.9, and 1.0 were determined:

$$\tau_{peak} = SL\,\tau_{static}, \tag{3}$$

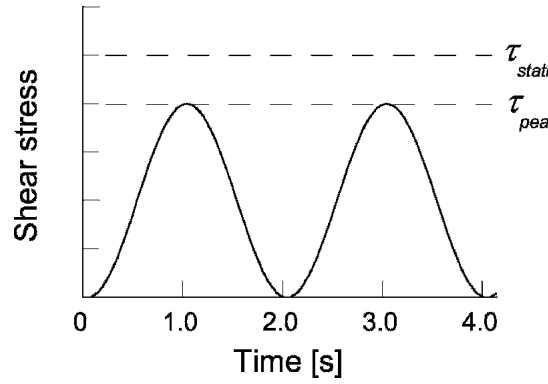

FIG. 6. Schema of stress waveform applied to the specimen in fatigue test.

where *SL* is the stress level, and τ_{static} is the mean static shear strength of test specimens for each group, as listed in Table 2. For each stress level, three to five specimens were used for every group in the fatigue test.

Shear strain, load, and the displacement of the actuator were recorded simultaneously with a dynamic data logger (PCD-1000, manufactured by Kyowa Electronic Instruments Co., Ltd., Tokyo, Japan) at a sampling frequency of 50 Hz. During the fatigue test, the strain gauge failed at a large number of loading cycles, after which shear strain was compared to the total deformation of the specimen calculated from the displacement of the actuator. All the tests were carried out at 24°C and relative humidity of 55%.

From these measurements, a hysteresis loop of the shear stress-strain curve was obtained for each loading cycle. The area enclosed by the hysteresis loop during one loading cycle was defined as the energy loss per cycle (U_c), which was calculated by numerical integration. The sum of energy loss from the first cycle to the number of cycles to failure (=fatigue life, N_f) was defined as cumulative energy loss at failure (U_{ac}). Mean energy loss per cycle (U_m) was calculated by dividing cumulative energy loss at failure (U_{ac}) by fatigue life (N_f).

RESULTS AND DISCUSSION

S-N diagram

Figure 7 shows the *S-N* diagrams for all specimens tested in the fatigue test. The vertical axis shows the stress level (*SL*) defined in Eq. (3), and the horizontal axis shows the number of cycles to failure, i.e., fatigue life (N_f). There exist negative linear relationships between stress level and fatigue life for each panel type and thickness on the semilogarithmic graph. Every regression line was statistically significant at the 1% significant level, as shown in Table 4. Then, regression lines were statistically compared by Analysis of Covariance (ANCOVA). First, ANCOVA was performed in each panel type to know the effect of panel thickness, that is, comparison between PW-9 and PW-12, and that between OSB-9.5 and OSB-12. There were no significant differences of regression lines between two different thicknesses in both PW and OSB: the probability corresponding to the F value was 0.79 for PW and 0.42 for OSB. Accordingly, regression analyses were conducted again for the combined data of PW-9 and PW-12, and those of OSB-9.5 and OSB-12. Regression lines for PW and OSB obtained irrespective of panel thickness were as follows: PW, $SL = 1.154 - 0.106 \log (N_f)$, $R^2 = 0.84$; OSB, $SL = 1.052 - 0.086 \log (N_f)$, $R^2 = 0.75$. ANCOVA was also performed between PW and OSB to know the effect of panel type. Fatigue life of PW was generally longer than that of OSB in higher stress levels as shown in Fig. 7, although no significant difference was obtained between the regression lines of PW and OSB: the probability corresponding to the F value was 0.052, which was slightly larger than the significant level of 0.05.

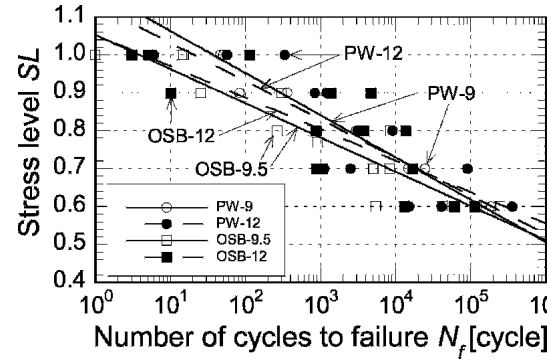

FIG. 7. Relationships between stress level (*SL*) and number of loading cycles to failure (N_f) for all specimens in fatigue test.

TABLE 4. *Results of regression analysis for the relationships between stress level and number of cycles to failure.*

Group	Regression equation	R^2	p-value
PW-9	$SL = 1.132 - 0.101 \log (N_f)$	0.98	<0.01**
PW-12	$SL = 1.175 - 0.111 \log (N_f)$	0.72	<0.01**
OSB-9.5	$SL = 1.053 - 0.090 \log (N_f)$	0.85	<0.01**
OSB-12	$SL = 1.053 - 0.083 \log (N_f)$	0.66	<0.01**

SL, stress level; N_f, number of cycles to failure; **, 99% significance

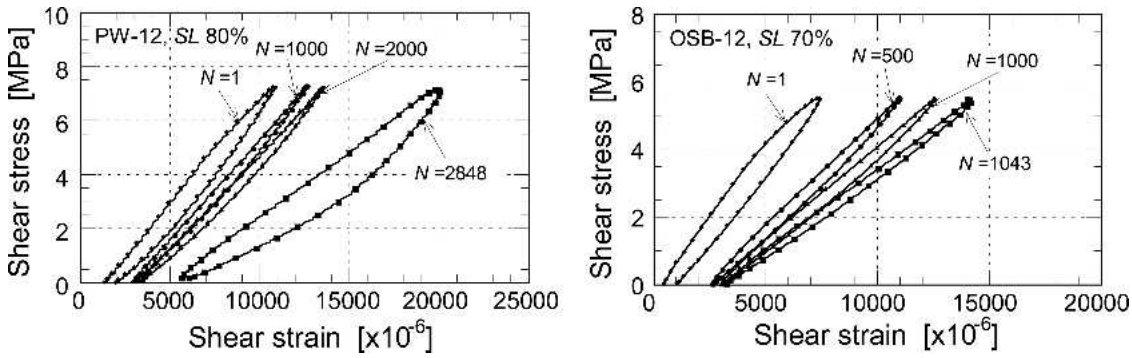

FIG. 8. Typical stress-strain curves under cyclic shear loading for PW-12 (left) and OSB-12 (right).

Stress-strain relationship

Figure 8 shows typical shear stress-strain relationships with increasing number of loading cycles (N) in the fatigue test. The left side shows the results for PW-12 at the stress level (SL) of 80%, and the right side those for OSB-12 at the stress level (SL) of 70%, as examples. As the number of loading cycles (N) increased, the slope of the stress-strain curve became gradually gentle, and maximum strain increased. These behaviors were seen in every specimen.

In addition, the area enclosed by the hysteresis loop, i.e., energy loss per cycle (U_c), changed during the fatigue test, as shown in Fig. 8. These changes are considered to be mainly due to the fatigue damage accumulated in the test specimens, as mentioned in the Introduction. The analysis of energy loss will reveal the development of fatigue damage in wood-based panels and possibly lead to the damage-based evaluation of fatigue properties of these panels, such as fatigue life and fatigue limit. We should, therefore, examine the relationships between energy loss and fatigue behavior of wood-based panels in the following sections.

Energy loss

Figure 9 shows the typical relationships between energy loss per cycle (U_c) and the number of loading cycles (N) for PW-12 and OSB-12. At each stress level (SL), the energy loss during the first cycle was almost twice as large as that during the second cycle. The energy loss during the first cycle was generally proportional to the stress level. These characteristics were commonly observed for all specimens. Because the wood-based panels are heterogeneous in their mechanical properties, their weak portions seem to be damaged during the first loading cycle. More portions are damaged at higher stress levels, which results in a larger energy loss. After

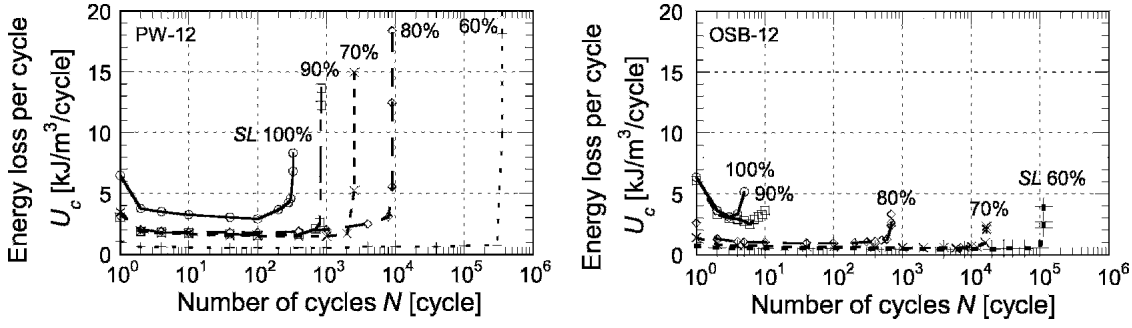

FIG. 9. Energy loss per cycle (U_c) under shear fatigue test for typical PW-12 (left) and OSB-12 (right) specimens.

the second loading cycle, the energy loss per cycle became approximately constant at each stress level, and it was larger at higher stress levels. The period in which energy loss per cycle was almost constant was a major part of fatigue life on logarithmic scale, as shown in Fig. 9.

Immediately before fatigue failure, the energy loss per cycle abruptly increased for both PW and OSB, as shown in Fig. 9. This result is similar to results obtained in other studies: solid wood in tension (Okuyama and Marsoem 1987), solid wood in tension-torsion and compression-torsion (Sasaki et al. 2005), and wood laminates in tension, compression, and tension-compression (Hacker and Ansell 2001). The energy loss immediately before fatigue failure was larger in PW than in OSB. The energy loss of PW was generally larger with a lower stress level, whereas that of OSB was almost the same at all stress levels. These results may be attributable to the components and composition of each panel. In the case of the static test, at the maximum load, PW underwent yielding, while OSB ruptured and broke apart, as shown in Fig. 4. This result indicates that PW seems to be ductile against catastrophic loading, whereas OSB is probably brittle in such an event. In fact, PW is made by "plane-gluing" several veneers together; on the other hand, OSB is made by "spot-gluing" many strands together. These structural differences may be responsible for the "ductility" of PW and the "brittleness" of OSB in their static breaking behaviors. In the fatigue test, PW also seemed to yield under catastrophic loading; hence, it underwent fatigue failure with several cycles of loading. PW was damaged more gradually at lower stress levels, which resulted in larger energy loss at fatigue failure. On the other hand, OSB seemed to break apart with approximately one cycle of catastrophic loading in the same manner as in the static test. Consequently, the energy loss of OSB at fatigue failure was considered to be almost the same at all stress levels.

As mentioned above, the changes in energy loss per cycle with repeated shear load could be divided into three stages: relatively large energy loss during the first cycle, constant energy loss after second loading cycle, and rapidly increasing energy loss just before fatigue failure. The second stage, in which the energy loss was almost constant, constituted the most part of fatigue life on logarithmic scale, as shown in Fig. 9. This result suggests that the logarithmic span of second stage is possibly a determining factor of logarithmic fatigue life. Accordingly, damage development in test specimen during the second stage may affect its fatigue life predominantly. Therefore, it was examined in the next section whether the fatigue behavior of the wood-based panel in the second stage is related to its fatigue life or not.

Fatigue life

In the previous section, it was shown that the energy loss per cycle in the second stage was almost constant, and that its magnitude depended on the stress level, as shown in Fig. 9. Fatigue life also depended on the stress level, as shown in Fig. 7. The relationship between energy loss in the second stage and fatigue life is discussed in this section. The average energy loss per cycle was obtained in the initial period of the second stage, that is, from the 5th to 10th loading cycles, and was defined as initial energy loss (U_i).

Figure 10 shows the relationships between initial energy loss (U_i) and fatigue life (N_f) for all specimens. There were significant correlations between initial energy loss and fatigue life on the semilogarithmic graph for both PW and

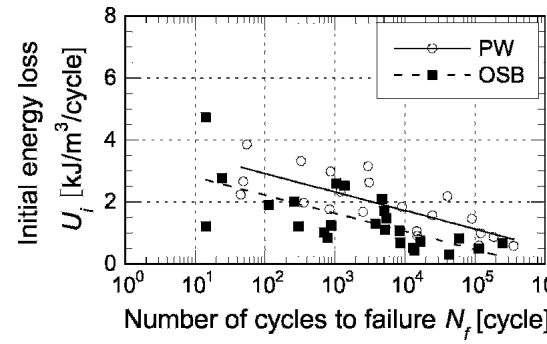

FIG. 10. Relationships between initial energy loss (U_i) and fatigue life (N_f) for all specimens in fatigue test.

OSB. The results of regression analysis are listed in Table 5. These results indicate that a wood-based panel with a smaller initial energy loss has a longer fatigue life. Therefore, fatigue life could be predicted using the regression equations given in Table 5 when energy loss per cycle is monitored during only a few loading cycles. This prediction method of fatigue life proposed here is considered to be very easy, quick, and probably nondestructive; the conventional fatigue test generally requires a long time as well as failure of the specimen in order to determine the fatigue life. This method could also be practically applied to the grading of full-sized wood-based panels for their fatigue life, though there are still many aspects that remain to be improved, such as the effects of the size difference between a test specimen and a full-sized panel on the fatigue behavior of these panels and the actual method of grading.

Fatigue limit

Energy loss per cycle was summed from the first cycle to a certain number of loading cycles, and plotted as a function of the number of loading cycles (N) in Fig. 11. For example, the plot on the 10^2 loading cycles exhibits the sum of energy loss from the first cycle to 10^2 loading cycles. The sum of energy loss from the first cycle to fatigue life (N_f) was the cumulative energy loss at failure (U_{ac}), as defined in the Materials and Methods, which is shown by the mark (×) in Fig. 11. The sum of energy loss was initially almost constant with increasing number of cycles, but later started to sharply increase. This tendency was observed in all specimens.

TABLE 5. *Results of regression analysis for the relationships between energy loss and number of cycles to failure.*

	Regression equation	R^2	p-value
$U_i - N_f$ (Fig. 10)			
PW	$U_i = 4.116 - 0.596 \log (N_f)$	0.60	<0.01**
OSB	$U_i = 3.390 - 0.584 \log (N_f)$	0.47	<0.01**
$U_{ac} - N_f$ (Fig. 12)			
PW	$U_{ac} = 7.246\ N_f^{0.850}$	0.94	<0.01**
OSB	$U_{ac} = 4.935\ N_f^{0.824}$	0.95	<0.01**

U_i, initial energy loss; U_{ac}, cumulative energy loss at failure; N_f, number of cycles to failure; **, 99% significance

Figure 12 shows the relationship between the cumulative energy loss at failure (U_{ac}) and the fatigue life (N_f) for all specimens. The results of regression analysis are listed in Table 5. We observed significant correlations between the two parameters on a double-logarithmic graph. The longer the fatigue life, the larger the cumulative energy loss at failure. In other studies on the fatigue of solid wood in tension (Marsoem et al. 1987) and solid wood in tension-torsion and compression-torsion (Sasaki et al. 2005), similar results were obtained—that cumulative energy loss at failure increased linearly as fatigue life became longer on a double-logarithmic graph. These results suggest that common characteristic features for the relationship between cumulative energy loss at failure and fatigue life are found in the fatigue behavior of wood and wood-based panels, though there has been some research on the fatigue in wood and wood composites by hysteresis analyses. Cumulative energy loss at failure reflects the fatigue damage accumulated up to failure. Therefore, further investigation on cumulative energy loss at failure may reveal the common fatigue failure mechanism for wood and wood composites.

Next, mean energy loss per cycle (U_m) was discussed in relation to the fatigue limit. Figure 13 shows the relationships between mean energy loss per cycle (U_m) and fatigue life (N_f) for all specimens on a semilogarithmic graph. As fatigue life becomes longer, mean energy loss per cycle decreases and gradually approaches a constant value, particularly in OSB. Okuyama et al. (1984) obtained a similar result that the mean energy loss per cycle of solid wood in cyclic tensile load or compressive load decreased and approached asymptotically constant values as the lifetime lengthened. These results represent that the fatigue life will be infinite when mean energy loss per cycle is below the constant value. Therefore, the constant value of mean energy loss per cycle is considered to be the threshold of whether the test specimen is damaged by one loading cycle or not. The stress level at which the mean energy loss per cycle is equal to the threshold value can be regarded as the fatigue limit. The fatigue limit of wood-based pan-

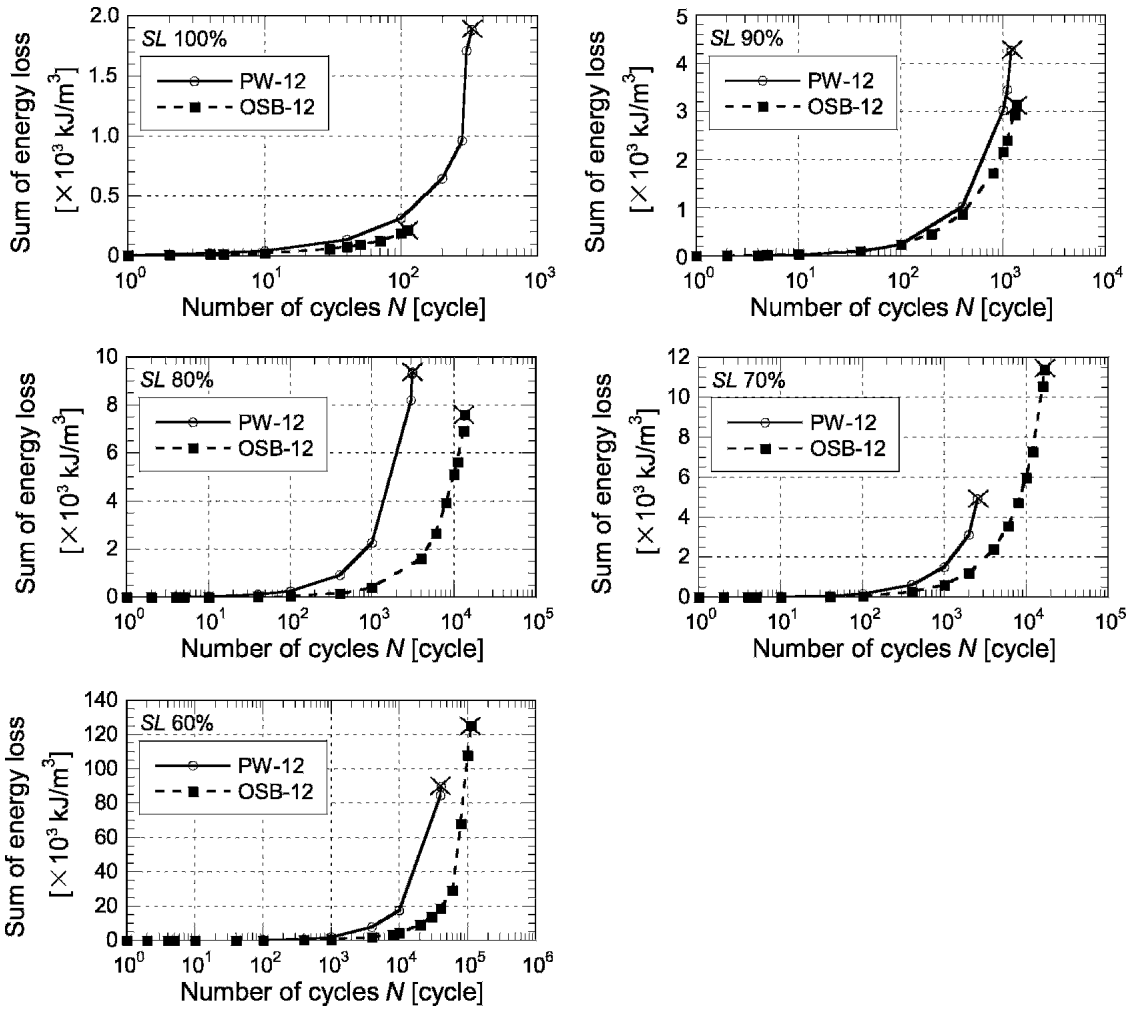

FIG. 11. Sum of energy loss under shear fatigue test for typical PW-12 and OSB-12 specimens. Each plot exhibits the sum of energy loss from the first cycle to the each number of loading cycles. The mark (×) indicates cumulative energy loss at failure.

els may be useful in designing timber structures, and hence is analyzed below.

In order to obtain the threshold value of mean energy loss per cycle, the following model equation between mean energy loss per cycle (U_m) and fatigue life (N_f) was proposed and fitted to the data shown in Fig. 13:

$$U_m = a\,\{1 + b\,\exp\,(-c\,\log\,(N_f\,))\}, \quad (4)$$

where a, b, and c are positive constant coefficients. a is the threshold value of mean energy loss per cycle because the exponential term in Eq. (4) is asymptotically zero when the fatigue life is infinite. The a values for PW and OSB were obtained to be 0.446 and 0.350 [kJ/m^3/cycle], respectively (see Table. 6). This result suggests that PW and OSB are probably undamaged below their respective threshold values of energy loss, and that energy loss below the threshold value might be considered to be mainly heat loss through internal friction of these panels.

The relationships between mean energy loss per cycle (U_m) and stress level (SL) for all speci-

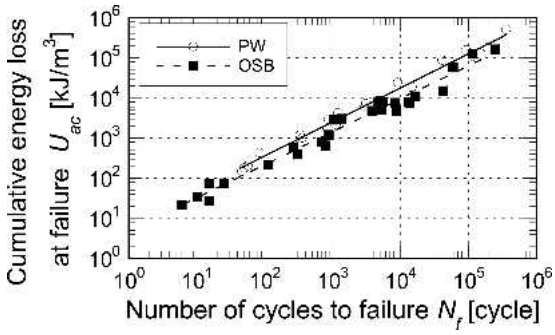

FIG. 12. Relationships between cumulative energy loss at failure (U_{ac}) and fatigue life (N_f) for all specimens in fatigue test.

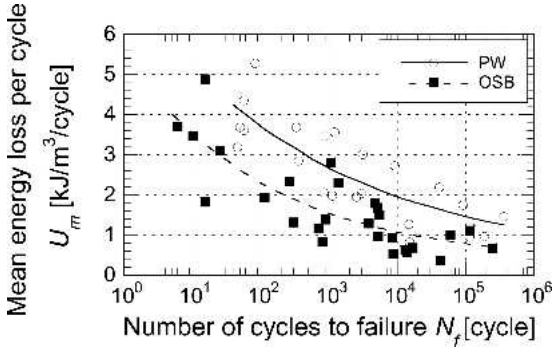

FIG. 13. Relationships between mean energy loss per cycle (U_m) and fatigue life (N_f) for all specimens in fatigue test.

mens are shown in Fig. 14. We found nonlinear relationships between these two parameters. When fatigue life is assumed to be infinite at the mean energy loss per cycle below 0.446 [kJ/m^3/cycle] for PW and 0.350 [kJ/m^3/cycle] for OSB, the fatigue limits of PW and OSB are evaluated to be 39% and 43% stress levels, respectively, by extrapolating the regression lines shown in

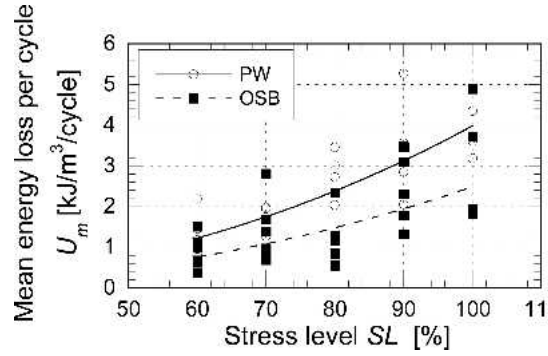

FIG. 14. Relationships between mean energy loss per cycle (U_m) and stress level (SL) for all specimens in fatigue test.

Fig. 14 and listed in Table 6. These results show that fatigue limits of both PW and OSB under shear load through the thickness are at almost the same stress level, that is, about 40%. There have been a few studies on the fatigue limit of wood-based panels: Bao et al. (1996) reported that the experimentally obtained fatigue limit is 30% to 40% of the average modulus of rupture (MOR) in the bending fatigue test for several kinds of wood-based panels. Their results and the results obtained in this study suggest that the fatigue limits of wood-based panels are likely to be at the same stress level regardless of panel type and loading type. On the other hand, wood-based panels have different static mechanical properties; in our present study, static strength in shear through thickness is higher for OSB than that for PW, as seen in Table 2. Similar results for static shear strength have already been reported in past studies on two-rail shear and edgewise shear tests for wood-based panels (Suzuki et al. 2000; Suzuki and Miyagawa 2003). The shear stress corresponding to the fatigue limit is,

TABLE 6. *Results of regression analysis for estimation of fatigue limit.*

	Regression equation	R^2
$U_m - N_f$ (Fig. 13)		
PW	$U_m = 0.446\ \{1 + 15.797\ \exp(-0.387\ \log\ (N_f)\ )\}$	0.60
OSB	$U_m = 0.350\ \{1 + 14.736\ \exp(-0.493\ \log\ (N_f)\ )\}$	0.47
$U_m - SL$ (Fig. 14)		
PW	$U_m = 9.902 \times 10^{-5}\ SL^{2.303}$	0.67
OSB	$U_m = 5.716 \times 10^{-5}\ SL^{2.320}$	0.44

U_m, mean energy loss per cycle; N_f, number of cycles to failure; SL, Stress level

therefore, larger in OSB than in PW. These results mean that OSB has higher performance than PW in not only static shear but also shear fatigue. One of the reasons why OSB has higher shear performance than PW could be that the strands in each layer of OSB are not completely oriented in contrast to the fiber direction in PW; some randomly oriented strands may have a beneficial effect on resistance to both static and cyclic shear load through the thickness.

As described above, analyses based on energy loss led to the elucidation of the fatigue limit of wood-based panels in shear through thickness. For solid wood, the fatigue limit in tension (Marsoem et al. 1987) and multiaxial-combined loading (Sasaki et al. 2005) was accurately estimated to be 25% of the static strength by analogous analyses based on energy loss. These analyses are useful because more labor and time are required to obtain the fatigue limit experimentally. To our knowledge, this is the first study to clarify the fatigue limit of wood-based panels under shear load through the thickness. The results are considered to be very important and useful for the design of timber structures. In particular, the fatigue limit, which is about 40% of the mean static shear strength, may provide a base value for determining the allowable design stress.

CONCLUSIONS

In the present study, fatigue tests on two types of wood-based panels (plywood and oriented strandboard) under shear load through the thickness were conducted, and the fatigue behavior was discussed mainly from the viewpoint of energy loss. The conclusions drawn are summarized below.

The change of energy loss per cycle with repeated shear load was divided into three stages: relatively large energy loss during the first cycle, constant energy loss after second loading cycle, and rapidly increasing energy loss just before fatigue failure. The energy loss in the initial period of the second stage showed a significant correlation with fatigue life, that is, a wood-based panel with a smaller initial energy loss has a longer fatigue life. Therefore, the fatigue life of specimens could be predicted by monitoring the energy loss per cycle in a test with several loading cycles. A model equation for the relationship between mean energy loss per cycle and fatigue life was proposed, and the threshold value of mean energy loss per cycle was obtained for the fatigue limit. Then, the fatigue limit of plywood and oriented strandboard was estimated to be approximately 40% of each static shear strength, on the basis of the relationship between mean energy loss per cycle and stress level. In terms of the absolute stress value, the oriented strandboard has higher shear performance than plywood in not only static but also fatigue in shear through thickness.

The results obtained in this study could provide valuable information for the design of timber structures, and additionally, give a greater utility value to wood-based panels in the case of new applications. We note here that the cyclic shear loading test through the thickness in this study was conducted under one load condition, i.e., no reversed loading with sinusoidal waveform at a frequency of 0.5 Hz. In reality, wood-based panels are subjected to various load conditions during service. Therefore, it is necessary to demonstrate the effects of load conditions such as loading frequency and loading waveform on the fatigue behavior of wood-based panels under shear load through the thickness.

REFERENCES

ASTM D2719. 2001. Standard test method of structural panels in shear through-the-thickness. Section-7, Vol. 04.10. Wood. 399–402. American Society for Testing and Materials, West Conshohocken, PA.

BAO, Z., AND C. A. ECKELMAN. 1995. Fatigue life and design stresses for wood composites used in furniture. Forest Prod. J. 45(7/8):59–63.

———, ———, AND H. GIBSON. 1996. Fatigue strength and allowable design stresses for some wood composites used in furniture. Holz Roh- Werkst. 54:377–382.

BONFIELD, P. W., C. L. HACKER, M. P. ANSELL, AND J. M. DINWOODIE. 1994. Fatigue and creep of chipboard. Part 1, Fatigue at R = 0.01. Wood Sci. Technol. 28:423–435.

FALK, R. H., D. VOS, AND S. M. CRAMER. 1999. The comparative performance of woodfiber-plastic and wood-

based panels. Pages 269–274 *in* Proc. Fifth International Conference on Woodfiber-Plastic Composites.

HACKER, C. L., AND M. P. ANSELL. 2001. Fatigue damage and hysteresis in wood-epoxy laminates. J. Mater. Sci. 36:609–621.

GONG, M., AND I. SMITH. 2003. Effect of waveform and loading sequence on low-cycle compressive fatigue life of spruce. J. Mater. Civil. Eng. 15(1):93–99.

KOHARA, M., AND T. OKUYAMA. 1993. Mechanical responses of wood to repeated loading VI—Energy-loss partitioning scheme to predict tensile fatigue lifetime. Mokuzai Gakkaishi 39(11):1226–1230.

LEE, A. W. C., AND C. B. STEPHENS. 1988. Comparative shear strength of seven types of wood composite panels at high and medium relative humidity conditions. Forest Prod. J. 38(3):49–52.

MARSOEM, S. N., P. A. BORDONNÉ, AND T. OKUYAMA. 1987. Mechanical responses of wood to repeated loading II—Effect of wave form on tensile fatigue. Mokuzai Gakkaishi 33(5):354–360.

OKUYAMA, T., AND S. N. MARSOEM. 1987. Mechanical responses of wood to repeated loading IV—Temperature-rises due to energy-loss. Mokuzai Gakkaishi 33(11): 844–850.

———, A. ITOH, AND S. N. MARSOEM. 1984. Mechanical responses of wood to repeated loading I—Tensile and compressive fatigue fractures. Mokuzai Gakkaishi 30(10):791–798.

PRITCHARD, J., M. P. ANSELL, R. J. H. THOMPSON, AND P. W. BONFIELD. 2001a. Effect of two relative humidity environments on the performance properties of MDF, OSB, and chipboard. Part 1. MOR, MOE and fatigue life performance. Wood Sci. Technol. 35:395–403.

———, ———, ———, AND ———. 2001b. Effect of two relative humidity environments on the performance properties of MDF, OSB, and chipboard. Part 2. Fatigue and creep performance. Wood Sci. Technol. 35: 405–423.

SASAKI, Y., M. YAMASAKI, AND T. SUGIMOTO. 2005. Fatigue damage in wood under pulsating multiaxial-combined loading. Wood Fiber Sci. 37(2):232–241.

SHRESTHA, D. 1999. Shear properties tests of oriented strandboard panels. Forest Prod. J. 49(10):41–46.

SUZUKI, S., AND H. MIYAGAWA. 2003. Effect of element type on the internal bond quality of wood-based panels determined by three methods. J. Wood Sci. 49:513–518.

———, D. NAWA, K. MIYAMOTO, AND T. SHIBUSAWA. 2000. Shear-through-thickness properties of wood-based panels determined by the two-rail shear and the edgewise shear methods. J. Soc. Mat. Sci. Jpn. 49(4):395–400.

THOMPSON, R. J. H, M. P. ANSELL, P. W. BONFIELD, AND J. M. DINWOODIE. 2002. Fatigue in wood-based panels. Part 1: The strength variability and fatigue performance of OSB, chipboard and MDF. Wood Sci. Technol. 36:255–269.